Nature Environment and Pollution Technology
An International Quarterly Scientific Journal

p-ISSN: 0972-6268
(Print copies up to 2016)
e-ISSN: 2395-3454

Vol. 23 | No. 2 | pp. 979-989 | 2024

Original Research Paper

https://doi.org/10.46488/NEPT.2024.v23i02.032

Open Access Journal

Eco-Engineered Low-Cost Carbosorbent Derived from Biodegradable Domestic Waste for Efficient Total Chromium Removal from Aqueous Environment: Spectroscopic and Adsorption Study

Vandana Saxena*, Ashish Kumar Singh, Atul Srivastava*** and Anushree Srivastava*†**

*Department of Applied Science and Humanities, IIMT College of Engineering, Greater Noida, India

**Department of Mechanical Engineering, IIMT College of Engineering, Greater Noida, India

***Centre of Environmental Science, Institute of Interdisciplinary Studies, University of Allahabad, Prayagraj, Uttar Pradesh, India

†Correspondence author: Anushree Srivastava; anushree.srivastava12@gmail.com

Nat. Env. & Poll. Tech.
Website: www.neptjournal.com

Received: 12-10-2023
Revised: 08-12-2023
Accepted: 22-12-2023

Key Words:
Chromium
Bio-adsorption
Biodegradable waste
Groundwater

ABSTRACT

Chromium contamination in water bodies poses severe risks to both the environment and human health. This research introduces an innovative solution to this challenge by creating a vapor-activated carbosorbent from biodegradable household waste. The efficacy of this adsorbent in removing total chromium through batch methods from aqueous solutions was investigated. Surface analysis using scanning electron microscopy (SEM) exhibited a porous structure, while Fourier-transform infrared spectroscopy (FTIR) identified distinct functional groups on the surface. The point of zero charge (PZC), determined at 6.95, revealed the adsorbent's surface chemistry. Impressively, the synthesized carbosorbent exhibited significant adsorption capacities of 23.08 $mg.g^{-1}$ for Cr(III) and 24.84 $mg.g^{-1}$ for Cr(VI) under optimal conditions. The Langmuir isotherm model illustrated a monolayer adsorption mechanism aligned with the pseudo-second-order kinetic model, confirming chemisorption. Thermodynamic analysis disclosed favorable and spontaneous chromium adsorption. Negative $\Delta G°$ values affirmed the spontaneity, while the exothermic nature of the process was signified by the positive $\Delta H°$ value, indicating heat release. Increased randomness at the solid-liquid interface, indicated by the positive $\Delta S°$ value, underscored the enhanced affinity between the adsorbent and adsorbate. This study exemplifies the potential of the vapor-activated carbosorbent as an efficient and sustainable remedy for chromium-contaminated water bodies.

INTRODUCTION

Chromium is a potentially toxic element resulting from contemporary anthropogenic activity, which causes direct environmental problems with severe hazards to human beings (Mohanty et al. 2023). Meanwhile, the uncontrolled discharge of chromium into water bodies results in the heavy contamination of aquifers, which are one of the major sources of drinking water (Perraki et al. 2021). The presence of Cr(VI) in groundwater resources must be understood to assess the risks to human health (Vasileiou et al. 2019). In water bodies, chromium exists in two oxidation states, namely trivalent chromium (Cr(III)) and hexavalent chromium (Cr(VI), and their predominance is majorly dependent upon the pH of the aqueous system). At acidic pH, trivalent chromium occurs as a cation that is dominated by insoluble hydroxide complexes, and hexavalent chromium exists in oxyanions forms of dichromate ($Cr_2O_7^{2-}$) and monovalent chromate ($HCrO_4$).However, the alkaline pH supports the existence of divalent chromate ($Cr_2O_4^{2-}$) in water bodies (Anthony et al. 2021). Generally, Cr(VI) is more water soluble and thus more mobile in groundwater. Cr(III) is relatively unstable but still dangerous, while Cr(VI) is very stable and easily oxidized and potentially hazardous to the environment as it is toxic, teratogenic, and carcinogenic by accumulating into cells through easy penetration by cell membranes (Qiu et al. 2020). According to the World Health Organization (WHO), the permissible limit for chromium in drinking water is 50 ppb. At the same time, various parts of the world reported chromium toxicity due to the consumption of contaminated drinking water (Vaiopoulou & Gikas 2020). A variety of technologies can be employed for chromium removal from water bodies, such as reverse osmosis, photodegradation, adsorption, coagulation, electrochemical, biochemical degradation, and ion exchange (Nur-E-Alam et al. 2020,

Karimi-Maleh et al. 2021, GracePavithra et al. 2019). Traditionally, the conversion of hexavalent chromium into trivalent chromium has become the most common method for water treatment (Hackbarth et al. 2016). However, this method is accompanied by the problem of high concentrations of Cr(III) after treatment (Staszak et al. 2023). Adsorption is considered a very simple, economical, and effective technique for the complete removal of total chromium from an aqueous environment (Mallik et al. 2022). Due to their structural heterogeneity, activated carbon and biochar make excellent adsorbents for water remediation. These adsorbents bear different sizes of pores, such as macropores, mesopores, and micropores, which makes them a suitable candidates for the adsorptive removal of pollutants (Islam et al. 2019). Adsorption on activated carbons (AC) is an efficient and most applied technique to treat contaminated water. There are numerous studies reported the application of activated carbons for water treatment (Ugwu & Agunwamba 2020, Yahya et al. 2020, Zhao et al. 2020). Dong et al. (2023) developed a porous biochar using waste collected from the liquor industry in order to decontaminate hexavalent chromium from an aqueous solution. They found that the adsorptive behavior of the alkali activated biochar has 144.5mg.g^{-1} of adsorption capacity at optimum experimental conditions. The study further explained the mechanism of adsorption that suggested multilayer sorption with physical as well as chemical interaction occurring at the surface of the adsorbent (Dong et al. 2023). Another study was conducted by Chakraborty and Das (2023), where they developed a nano silica-coated biochar for the removal of hexavalent chromium from an aqueous solution that showed a maximum adsorption capacity of approximately 80mg.g^{-1}. The nanocomposite they prepared was examined at various experimental conditions to understand the mechanism of adsorption. The isothermal modeling and statistical analysis were well utilized in the research work that suggested validation of experimental data obtained during the study (Chakraborty & Das 2023). Similarly, Azaiez et al. studied the adsorptive removal of hexavalent chromium by using biochar, which was modified with zinc chloride. The result revealed an enhanced adsorption capacity of 177.64 mg.g^{-1} after modification. The high adsorption efficiency was obtained at extremely acidic conditions, which suggested its applicability to tannery water (Khalifa et al. 2023). However, traditional types of AC can be expensive to synthesize and may not always be energy efficient. Biomaterial-based adsorbents, on the other hand, can be effective and cost-efficient for decontaminating water. Moreover, converting waste biomass into value-added products has gained significant attention due to its renewability, environmental friendliness, and availability. To optimize the preparation of biochar, various methods can be used, such as physical activation, which involves temperature variation, and vapor activation, which can enhance its pore size distribution and surface area. Additionally, chemical activation using acids, alkalis, and metal oxides can be an effective way to modify the properties of biochar and improve its suitability for water decontamination. Overall, this study aimed to investigate the efficiency of using the prepared carbosorbent for adsorbing Cr(III) and Cr(VI) ions under different conditions, which can be useful for designing effective water treatment strategies

MATERIALS AND METHODS

Characterization of Carbosorbent

The surface morphology of the prepared biochar was examined using a scanning electron microscope (SEM) provided by Philips, Netherlands. Furthermore, to investigate the involvement of functional groups in the adsorption process, an attenuated total reflectance Fourier-transform infrared (ATR-FTIR) spectrometer with a resolution of 4 cm^{-1}, specifically the Nicolet 6700 model from Thermo Scientific in MA, USA, was utilized. This characterization technique allowed for a comprehensive analysis of the functional groups present in the carbosorbent. Further, the point of zero charge (PZC) of the adsorbent was determined by the mass titration method reported by method from the literature. In brief, 25 mL of 0.1 M NaCl solutions were prepared in separate flasks, and their initial pH values were adjusted to a range of pH 3.00 to 11.00 by the addition of suitable quantities of 0.1 M HCl or NaOH solutions. Subsequently, 0.1 g of the carbosorbent was introduced into each flask, followed by continuous stirring for approximately 24 h at room temperature using a shaker. After the 24-hour stirring period, the final pH of each flask was measured, and the difference between the final and initial pH values was recorded. By plotting the ΔpH (difference in pH) against the initial pH, the PZC values were determined.

Adsorption Experiment by Batch Method

The adsorption process of trivalent and hexavalent chromium ions using the prepared carbosorbent was examined using a systematic procedure. To experiment, a 25 mL solution was placed in a 100 mL conical flask containing 10mgL^{-1} of Cr(III) and Cr(VI) with different pH ranges from 3 to 12 and placed at a magnetic stirrer with a rotation speed of 100 rpm. Additionally, the adsorption tests were performed at room temperature with a contact time of 60 min and an adsorbent dosage of 2 g.L^{-1}. After each test, the carbosorbent was separated from the solution, and the concentration of the hexavalent and trivalent chromium was estimated. Similarly, the batch adsorption experiments for

under different environments, such as initial concentration (10–50 mgL^{-1}), adsorbent dosage (0.25–2.2 $g.L^{-1}$), contact time (10–120 min), and temperature (28–50°C), were performed to evaluate the optimum condition for maximum adsorption capacity of the prepared carbosorbent. The equations (1) and (2) were used to calculate the adsorption efficiency and adsorption capacity for Cr(III) and Cr(VI)

$$\% \, Sorption = \frac{C_i - C_e}{C_i} \times 100 \quad \ldots(1)$$

$$q_e \left(\frac{mg}{g}\right) = \frac{C_i - C_e}{M} \times V \quad \ldots(2)$$

Where C_i and C_e are the initial and final concentrations of the adsorbate, m is the mass of the adsorbent used, v is the volume in liter, and q_e is the maximum adsorption capacity of the developed adsorbent.

A UV-visible spectrophotometer determined the residual concentration of hexavalent chromium. (Systronic 2206) through the diphenyl carbazide method adopted by Kassimu et al. (2022). Briefly, 1 mL of treated solution mixed with 2N sulphuric acid followed by 100 µL of DPC stock solution prepared by dissolving 50 mg of 1,5 diphenyl carbazide in 25 mL acetone. An addition of DPC develops a reddish-violet color by forming a complex with Cr(VI). The intensity of color was examined at 540 nm to calculate the concentration of hexavalent chromium. The calibration curve was obtained with a standard solution of hexavalent chromium having a concentration of 10 to 50 mgL^{-1}. Meanwhile, trivalent chromium was estimated by determining total chromium with a Flame atomic absorption spectrophotometer (NOAA 350 F-AAS) equipped with acetylene and N_2O gas.

RESULTS AND DISCUSSION

Characterization by SEM, FT-IR, and PZC

The surface morphology of the vapor-activated carbosorbent was analyzed by scanning electron microscope (SEM) and presented in Fig. 1. The surface topography of the material displayed a significant level of heterogeneity with uneven distribution of pores, resulting in a high surface area. An ATR-FTIR study was employed to analyze the stretching and vibration of functional groups present on the surface of vapor-activated carbosorbent and presented in Fig. 2(a). The result revealed variations in the stretching, bending, and ionic vibrations of different functional groups at distinct wavenumbers. The adsorption process is notably affected by the presence of various functional groups, including carboxyl, hydroxyl, sulfate, and amino groups, etc. on the surface of the adsorbent (Bagheri et al. 2020). These functional groups play a crucial role in determining the adsorption capacity and efficiency of the material. The peak detected at approximately 3500 cm^{-1} signifies the presence of OH groups within the sample, while the peak observed in the range of 2900-2970 cm^{-1} signifies the interaction

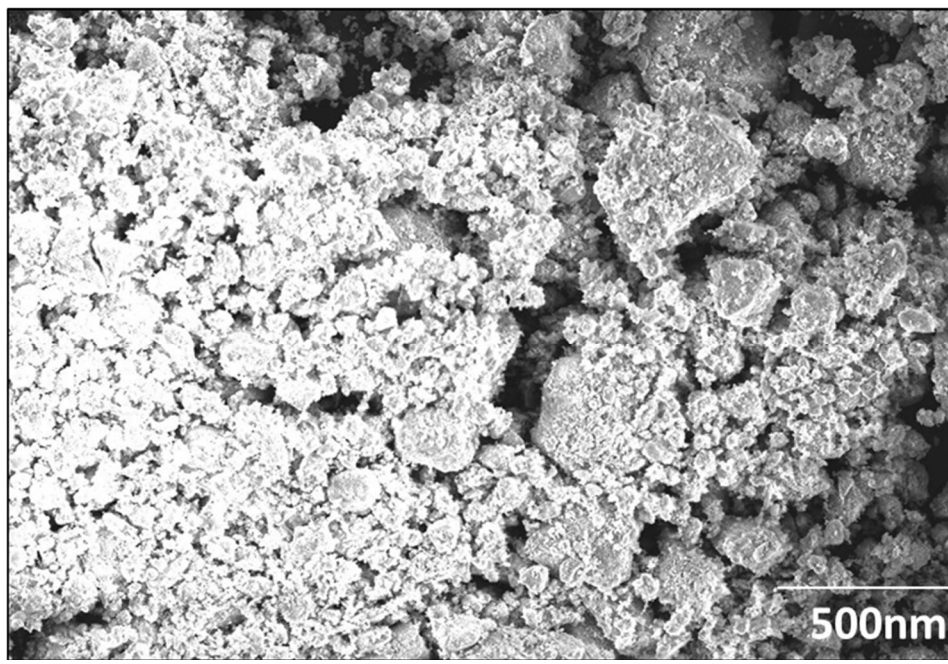

Fig. 1: SEM image of the vapour-activated carbosorbent developed from biodegradable domestic waste.

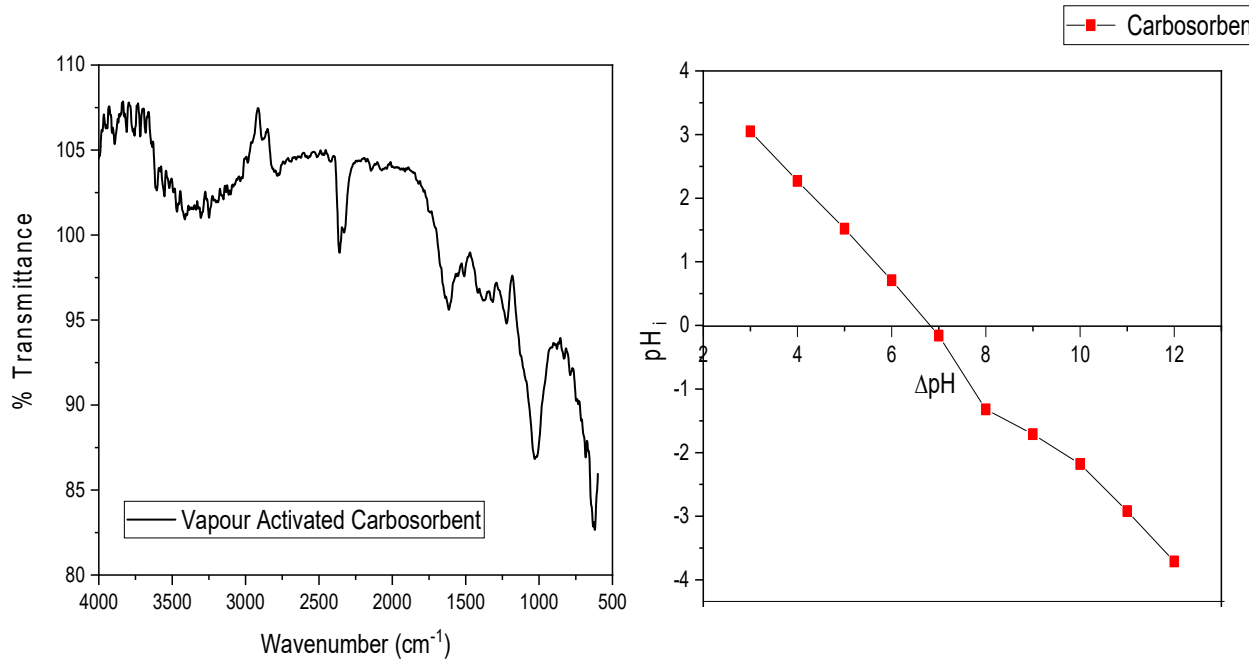

Fig. 2: (a) FTIR spectra of the developed carbosorbent (b) A graph between pH_i versus ΔpH to obtained point of zero charge (PZC).

between C-H bonds and the biochar surface (Zolfi Bavariani et al. 2019). Similarly, the presence of peaks near 1600 cm^{-1} indicates the presence of amides, which can be discerned on the surface of the carbosorbent.

Additionally, the well-defined peak at approximately 1700 cm^{-1} provides evidence for the presence of a carbonyl group (Srivastava et al. 2022a). This peak can be attributed to various functional groups, such as carboxyl groups (-COOH) from organic acids or ester groups (-COOR) from polysaccharides (Adeniyi et al. 2020). Furthermore, the peaks observed around 1200 and 1000 cm^{-1} likely originate from the stretching and vibration involving N-H bonds (Srivastava et al. 2020).

Moreover, peaks in the region of 1000-1300 cm^{-1} are often observed, which are associated with the stretching vibrations of C-O and C-O-C bonds, indicating the presence of polysaccharides or other organic compounds (Hu et al. 2022). The surface chemistry of the adsorbent was also investigated by measuring the pH at the point of zero charge (pHzpc).A graph plotted between ΔpH versus pHi where 6.95 of PZC was obtained at section point and presented in Fig. 2(b). The observed neutral pH at the point of zero charges (pHzpc) on the carbosorbent implies the presence of substantial surface groups capable of either consuming or releasing H^+ (Yadav et al. 2023). These groups are likely to be -OH groups, which can exert a notable influence on the adsorptive behavior of the carbosorbent (Andrade et al. 2020).

Effect of pH and Initial Concentration

The pH of a solution exerts a substantial influence on the adsorption of an adsorbate, as it governs critical parameters such as surface charge, ionization degree, and ion speciation. The graph in Fig. 3(a) presents the adsorption data for total chromium removal, specifically examining the impact of pH values ranging from 3 to 9. The experimental setup included using 0.05 g of the adsorbent in a 25 mL test solution with a contact time of 60 to 120 min and a shaking speed of 150 rpm at room temperature. The outcomes of the analysis indicate that the adsorption efficiency of both Cr(III) and Cr(VI) increases concurrently with increasing pH, attaining its peak at pH 7. However, beyond this optimal pH point, a gradual decrease in efficiency is observed. Remarkably, at pH 7, an exceptionally high adsorption percentage of 99.02% was achieved for Cr(III), while Cr(VI) exhibited an even more impressive adsorption rate of 99.18%.

Conversely, an analysis of the adsorption process at the initial pH of 3 revealed significantly inferior efficiency figures of 35.21% (Cr(III)) and 40.75% (Cr(VI)). These findings emphasize that extremely acidic pH conditions negatively impact the adsorption of chromium ions due to electrostatic repulsion between the adsorbate and adsorbent. In a neutral environment, chromium species exist as oxyanions, which release hydrogen atoms as the pH increases(Sarkar et al. 2019). These oxyanions then interact with hydroxyl sites on the adsorbent, resulting in improved adsorption efficiency

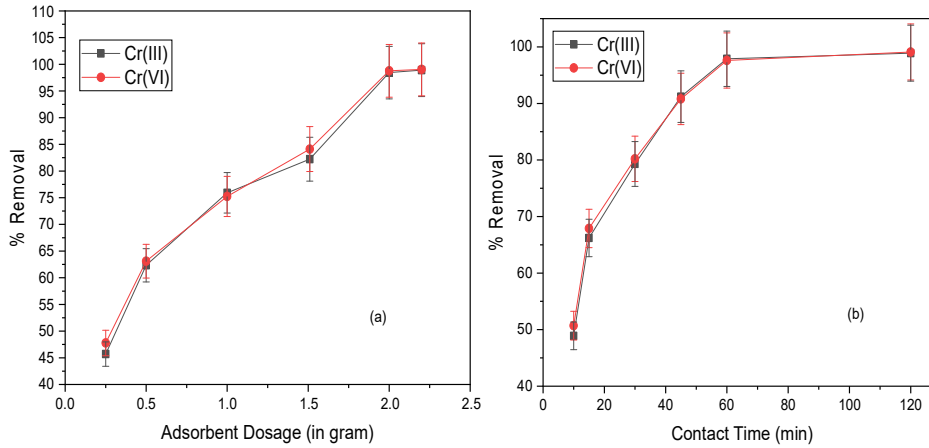

Fig. 3: (a) Effect of pH on the adsorptive removal of trivalent and hexavalent chromium (b) Effect of initial concentration for the removal of total chromium from aqueous solution.

(Chen et al. 2011). However, under alkaline conditions, the presence of competing hydroxide ions reduces adsorption by occupying available sites on the adsorbent surface, thereby hindering the attachment of chromium ions. The observed successive decrease in the percentage removal of Cr ions at lower and higher pH suggests the potential saturation of the binding capacity of the adsorbent (Wan et al. 2023). The findings of this study support previous reports indicating a favorable neutral pH range for chromium removal (Pap et al. 2018, Zhao et al. 2018). However, it is noteworthy that certain researchers have also highlighted the potential of acidic pH levels in effectively removing hexavalent chromium (Gupta et al. 2018, Shakya et al. 2019). The effect of initial concentration on the removal efficiency of total chromium was also examined using a prepared carbosorbent at various predetermined chromium concentrations ranging from 10 to 50 $mg.L^{-1}$ and presented in Fig. 3(b). Initially, the adsorption and removal rate of chromium solution by the carbosorbent achieved a remarkable 99.3% and 99.5% efficiency for Cr(III) and Cr(VI) ions, respectively. However, as the initial concentration increased, the removal rate declined due to a decrease in available active sites necessary to accommodate higher ion concentrations. In contrast, the adsorption capacity exhibited a rapid increase owing to the intensified adsorption driving force resulting from the higher solution concentration. This facilitated improved contact between the adsorbent and adsorbate. At an initial concentration of 50 mg/L of chromium ions solution, the removal rate of 83.5% and 84.49% for Cr^{3+} and Cr^{6+} suggests that the adsorption of chromium ions by the carbosorbent approached equilibrium when the initial concentration reached 50 $mg.L^{-1}$. Alternatively, this trend could be attributed to the saturation of active sites on the adsorbent at higher chromium concentrations. Consequently, the decline in the percentage removal of chromium can be ascribed to either the limited binding capacity of the adsorbent or the occupation of active sites by chromium ions (Jamaluddin et al. 2022).

Effect of Adsorbent Dosage and Contact Time

The dosage of adsorbent used for ion uptake played a significant role in adsorption, as illustrated in Fig. 4(a). Under neutral pH conditions and an initial chromium concentration of 10 $mg.L^{-1}$, a biochar dosage of 2 $g.L^{-1}$ achieved a remarkable removal efficiency of approximately 99% for total chromium. However, as the mass of biochar increased, both the adsorption amounts and the adsorption per unit mass of adsorbent decreased despite the constant initial concentration of the solution. The initial increase in removal rate with higher adsorbent mass can be attributed to the availability of more binding sites for adsorption. Nevertheless, further increases in adsorbent mass did not impact the removal rate, indicating the saturation of adsorbate sites by chromium ions and their subsequent unavailability (Birhanu et al. 2020). The study also investigated the influence of contact time on the adsorption process and, presented in Fig. 4(b). The result indicated that the adsorption of total chromium increased as the contact time between the carbosorbent and the solution was prolonged. A saturation point was reached after 60 minutes, indicating that further contact time did not lead to significant additional adsorption.

Interestingly, a substantial amount of chromium ions was adsorbed within the initial 30 minutes of contact time, suggesting that a shorter duration may be sufficient for efficient chromium removal using the carbosorbent. Furthermore, the research observed no notable changes in the equilibrium condition beyond the 60-minute mark, up to

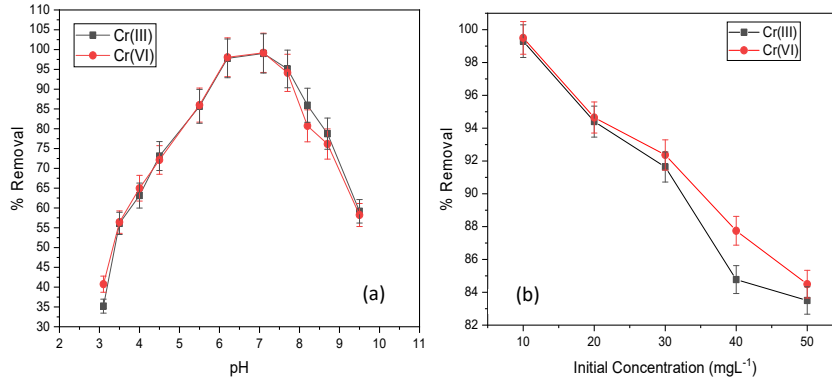

Fig. 4: Effect of adsorbent dosage (a) and effect of contact time (b) on adsorption of trivalent and hexavalent chromium onto vapor-activated carbon sorbent (total chromium-, 10mg/L, sorbate concentration: 2g/L at 30°C).

a maximum of 120 minutes. This suggests that the adsorption process achieved equilibrium within the initial 60 minutes of contact time. The reaction rate analysis revealed a rapid initial adsorption process, which can be attributed to the substantial concentration gradient between the adsorbate and the available vacant sites on the surface of the carbosorbent. However, as the experiment continued, the reaction rate gradually decreased. This decline can be attributed to a reduction in the number of vacant sites on the surface of the adsorbent, limiting the adsorption capacity over time (Bai et al. 2020).

Isothermal Modelling

Adsorption isotherms are mathematical models that describe how adsorbate molecules are distributed between liquid phases at various equilibrium concentrations (Dim et al. 2021). The two widely used models are the Langmuir and Freundlich models. In this study, both models were employed to establish the relationship between the number of adsorbed chromium ions and their equilibrium concentration in the solution. The Langmuir model proposes that adsorption takes place on a homogeneous surface with uniformly permeable and efficient regions. Consequently, a monolayer of adsorbate molecules is formed on the surface of the material, effectively saturating the available pores and hindering the mobility of additional molecules (Bedada et al. 2020).

The following formula can be used to define a non-linear expression of the Langmuir isotherm.

$$q_e = q_m K_L \frac{C_e}{1+K_L C_e} \quad \ldots(3)$$

Where,

q_e = the adsorption capacity

C_e = concentration of the adsorbate at equilibrium

K_L = Langmuir Constant (Lmg^{-1}), and q_m is the monolayer adsorption capacity in $mg.g^{-1}$

The maximum adsorption capacity of trivalent and hexavalent chromium by the vapor-activated carbosorbent was determined by a nonlinear curve plotted between q_e and C_e and represented in Fig.5(a). The monolayer adsorption capacity was found to be 23.08 $mg.g^{-1}$ and 24.84 $mg.g^{-1}$ for Cr(III) and Cr(VI), respectively. The plot also provided a strong correlation coefficient in both cases, denoting the monolayer sorption capacity in units of $mg.g^{-1}$ of the adsorbent. The adsorption energy, indicated by K_L with units of $L.mg^{-1}$, was also analyzed and provided in Table 1.

To assess the shape of the isotherm, a dimensionless constant called the separation factor (RL) was utilized. The R_L value can be calculated using the following equation:

$$R_L = \frac{1}{1+K_L C_i} \quad \ldots(4)$$

The value of the R_L parameter categorizes the isotherm into the following four types:

Irreversible isotherm ($R_L = 0$): This indicates a complete lack of adsorption, where the solute does not interact with the adsorbent.

Linear isotherm ($R_L = 1$): This suggests a uniform and proportional adsorption process, where the adsorbate concentration is directly related to the amount adsorbed.

Table 1: Comparative values of the parameters calculated for the removal of Cr(III) and Cr(VI) by equilibrium models.

Langmuir Isotherm				Freundlich Isotherm	
	Cr (III)	Cr (VI)		Cr (III)	Cr (VI)
Q_m [$mg.g^{-1}$]	23.08	24.84	K_f [$L.mg^{-1}$]	1.22	1.80
R^2value	0.957	0.952	R^2 Value	0.93	0.936
K_L [$L.mg^{-1}$]	0.63	0.57	1/n Value	0.293	0.281

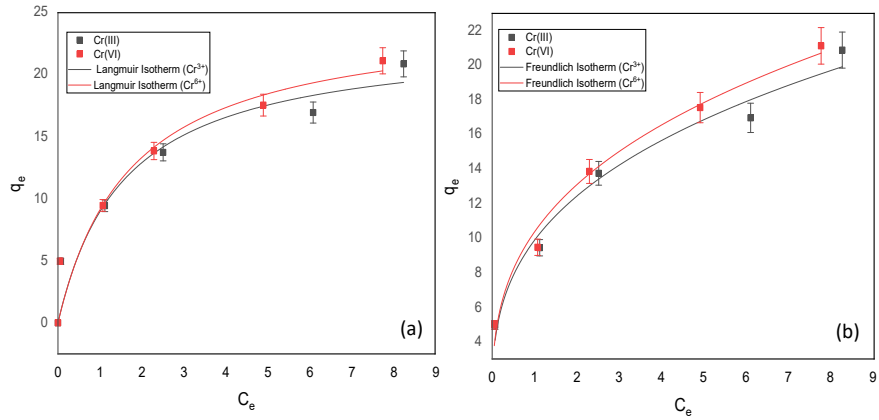

Fig. 5: Langmuir (a) and Freundlich (b) isotherm for adsorption of trivalent and hexavalent chromium onto vapor-activated carbosorbent.

Favorable isotherm ($0 < R_L < 1$): This signifies a favorable adsorption process, where the adsorbent exhibits a preference for the adsorbate. The R_L value between zero and one suggests efficient adsorption with a gradual decrease in the adsorption capacity as the concentration increases.

Unfavorable isotherm ($R_L > 1$): This indicates an unfavorable adsorption process, where the adsorbate faces resistance in interacting with the adsorbent. The R_L value greater than one implies a reduced affinity between the adsorbent and adsorbate as the concentration rises.

The estimated R_L values for Cr(III) and Cr(VI) ions are 0.136 and 0.149, respectively, which are less than one and larger than zero, indicating favorable adsorption (Tangestani et al. 2022). The application of the Freundlich isotherm model was employed to investigate the adsorption of total chromium ions in our research study. This model provides valuable insights into the adsorption process, indicating that it is non-ideal and reversible. It suggests that adsorption occurs through the formation of multilayers of the analyte on a heterogeneous surface with uneven characteristics (Srivastava et al. 2019). The non-linear expression of the isotherm is given as follows.

$$q_e = K_f C_e^{1/n} \quad \ldots(5)$$

The Freundlich equation is a widely used empirical model for describing the adsorption process of solute molecules onto a solid adsorbent surface. It incorporates two key parameters: the Freundlich constant (K_f) and the Freundlich exponent (n). The K_f value represents the relative adsorption capacity of the adsorbent, while the exponent (n) provides insight into the intensity of adsorption. Generally, an increase in the K_f value signifies a higher adsorption capacity of the adsorbent. Moreover, when the value of n falls within the range of 1 to 10, it indicates an effective adsorption process. (Dan & Chattree 2018) (Fig. 5b). The n value achieved in this study is better or equivalent to that of previously reported adsorbents for chromium removal(Jeyaseelan et al. 2021) (Ahamad et al. 2018). By comparing correlation coefficients (R^2), the suitability of isotherm models for the removal study was determined. Table 1 shows that both isotherm models correlate well with experimental data, although Langmuir's isotherm fits best with a higher correlation coefficient than the Freundlich isotherm. The maximum adsorption capacity (qm) obtained in the present study is better than apple wood biochar where qm was reported at 7.71mg.g^{-1}(Liu et al. 2020) Another study performed by Amin and Chetpattananondh for the removal of hexavalent chromium by using algal biochar showed 15.94mg.g^{-1} of monolayer adsorption capacity (Amin & Chetpattananondh 2019). Similarly, Rajapaksha et al. examined biochar developed with soybean for the removal of total chromium at acidic pH, where the maximum adsorption capacity was found to be 17.02 mg.g^{-1} (Rajapaksha et al. 2018)

Kinetic Modelling

Pseudo-first-order kinetics is commonly used to describe the adsorption process, assuming that the rate of adsorption is proportional to the difference between the saturation concentration and the amount of adsorbate adsorbed on the surface at a given time (Chakraborty et al. 2021).

The mathematical expression for the nonlinear pseudo-first-order kinetic model is:

$$q_t = q_e(1 - e^{-kt}) \quad \ldots(6)$$

Where :

q_t is the amount of adsorbate adsorbed at time t

q_e is the amount of adsorbate adsorbed at equilibrium

k_1 is the rate constant of pseudo-first-order kinetics

The pseudo-first-order kinetic model assumes that the

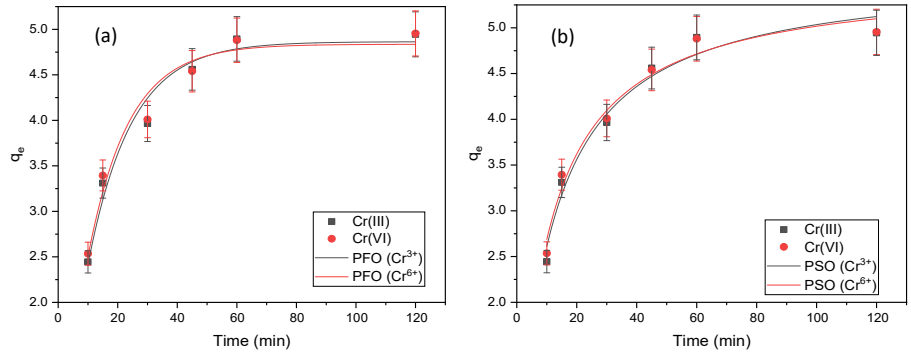

Fig. 6: Adsorption kinetic models for chromium ion uptake (a) pseudo-first-order model, (b) pseudo-second-order model for trivalent and hexavalent chromium onto vapor-activated carbosorbent.

Table 2: Kinetic parameter obtained for adsorption of Cr(III) and Cr(VI) onto vapor-activated carbosorbent.

Pseudo First Order			Pseudo Second Order	
	Cr (III)	Cr (VI)	Cr (III)	Cr (VI)
$K_1(min^{-1})$	0.072	0.073	0.010	0.025
R^2 value	0.922	0.925	0.974	0.976
q_e mg/g)	4.79	4.81	5.61	5.55

adsorption process is primarily controlled by the external mass transfer and the adsorbate concentration difference between the solution and the adsorbent surface (Revellame et al. 2020). A graph plotted between q_t and time for the adsorption study and presented in Fig. 6a. This model is often used for preliminary analysis or to estimate the rate constant of the adsorption process. However, it is important to note that the pseudo-first-order kinetic model may not always accurately describe the adsorption process. In some cases, the adsorption mechanism may be more complex, involving multiple steps or other factors that are not considered in this simplified model (Benjelloun et al. 2021). To gain a more comprehensive understanding of the adsorption process, it is common to examine the kinetics using the pseudo-second-order model as well. The mathematical expression for the nonlinear pseudo-second-order kinetic model is:

$$q_t = \frac{k_2 q_e^2 t}{1+k_2 q_e t} \quad \ldots(7)$$

Where k_2 is the rate constant of pseudo-second-order kinetics, the pseudo-second-order kinetic model was also plotted with q_t versus t, which provides a more accurate representation of the adsorption process, especially when the pseudo-first-order model fails to describe the experimental data adequately (Srivastava et al. 2021b) (Fig. 6b). The comparative data presented in Table 2 shows that the pseudo-second-order kinetic model exhibits a higher correlation coefficient compared to the pseudo-first-order model for both trivalent and hexavalent chromium. This indicates that the pseudo-second-order model provides a better fit to the experimental data and offers a more accurate explanation of the sorption kinetic behavior for chromium removal by carbosorbent. The higher correlation coefficient associated with the pseudo-second-order model suggests a stronger linear relationship between the observed and calculated values, indicating a closer agreement between the model and the actual data points(Srivastava et al. 2022b). Furthermore, the pseudo-second-order kinetic model, which represents a single-step rate-limiting process, confirms the chemical nature of the sorption of chromium ions on the carbosorbent.

Thermodynamic Study

To investigate the nature of the sorption process, an adsorption experiment was conducted at different temperatures (25, 34, 42, and 60°C). The objective was to determine the thermodynamic parameters that characterize the reaction occurring during the sorption process. These parameters were determined by evaluating the coefficient of distribution (K_D) at each temperature (Yusuff 2019). The coefficient of distribution (K_D) is a measure of the distribution of an adsorbate between two phases that provides insights into the equilibrium concentration of the adsorbate in each phase at a given temperature (Srivastava et al. 2021a). By performing the adsorption experiment at various temperatures and evaluating the K_D values, it becomes possible to analyze the effect of temperature on the sorption process and determine the corresponding thermodynamic parameters. These parameters can include the standard free energy change (ΔG°), the standard enthalpy change (ΔH°), and the standard entropy change (ΔS°) associated with the sorption reaction.

$$\ln K_D = \left(\frac{\Delta S^o}{T}\right) - \left(\frac{\Delta H^o}{RT}\right) \quad \ldots(8)$$

A graph was constructed to analyze the correlation between the coefficient of distribution (K_D) and inverse of temperature (Fig. 7) . This graphical representation allowed

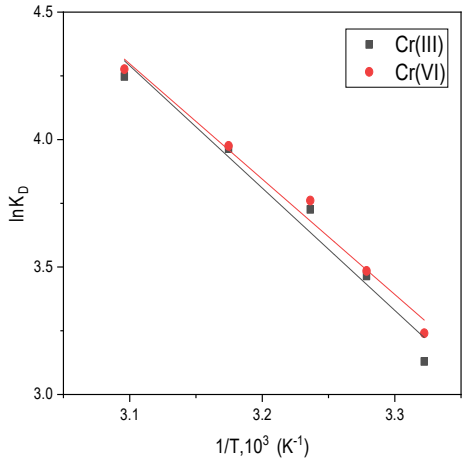

Fig. 7: Plot of ln K_D Vs. 1/T for the estimation of thermodynamic parameters for sorption of total chromium by carbosorbent.

Table 3: Thermodynamic parameters at various temperatures for the adsorption of Cr(III) and Cr(VI).

Temperature (in Kelvin)	Cr(III)		Cr(VI)	
301	ΔG° [KJ.mol^{-1}]		ΔG° [KJ.mol^{-1}]	
	-7.831	ΔH° = 33.82 J.mol^{-1}	-8.108	ΔH° = 37.57 J.mol^{-1}
305	-8.875	ΔS° = 159.29 J.mol^{-1}	-8.836	ΔS° = 152.31 J.mol^{-1}
309	-9.572		-9.661	
315	-10.382		-10.41	
323	-11.406		-11.48	

us to determine the change in Gibbs free energy (ΔG°) at different temperatures, a parameter that indicates the feasibility and spontaneity of the sorption process (Mpelane et al. 2022). The enthalpy change (ΔH°) and entropy change (ΔS°) were also computed using specific equations. These thermodynamic parameters presented in Table 3 shed light on the heat exchange and level of disorderliness occurring at the sorption interface (Jahangiri et al. 2019). The results demonstrated that the sorption process is feasible and spontaneous, as evidenced by the negative ΔG° values. Moreover, as the temperature increased, the sorption process became more favorable. For the adsorption of chromium ions, the process was confirmed to be thermodynamically spontaneous. The positive ΔH° value indicated that the sorption process is endothermic, implying the absorption of heat during the reaction (Abdel-Mohsen et al. 2020). Notably, the calculated enthalpy change (ΔH°) was found to be 39.82 kJ.mol^{-1} and 37.57 kJ.mol^{-1} for trivalent and hexavalent chromium, respectively, suggesting a chemical sorption mechanism due to its value exceeding 21 kJ.mol^{-1}. Additionally, the positive ΔS° value indicated an increase in the level of randomness at the solid-liquid interface during the sorption process (Srivastava et al. 2022c).

CONCLUSION

The vapour-activated carbosorbent developed using biodegradable domestic waste has proven to be effective in removing total chromium from aqueous solutions. The surface characterization of the prepared adsorbent BY SEM revealed its porous structure, while FTIR spectra showed possible functional groups that might play a crucial role in the adsorption process. Additionally, the surface chemistry of the adsorbent is explained by the point of zero charge, which was found to be 6.95. The synthesized carbosorbent exhibited an adsorption capacity of 23.08mg.g^{-1} and 24.84mg.g^{-1} for Cr(III) and Cr(VI), respectively, under optimal experimental conditions. The adsorption process followed the Langmuir isotherm model, indicating a monolayer adsorption mechanism, while the pseudo-second-order kinetic model confirmed that the adsorption reaction was of a chemisorption nature. The negative values of ΔG° (standard Gibbs free energy change) indicated that the adsorption process is spontaneous, suggesting favorable adsorption of total chromium onto the adsorbent. In addition, the positive value of ΔH° (standard enthalpy change) suggests an exothermic nature of the adsorption reaction, implying that heat is released during the process. The positive value of ΔS° (standard entropy change) indicates an increase in randomness at the solid-liquid interface during the adsorption of chromium ions, indicating an improved affinity between the adsorbent and the adsorbate. Overall, the combination of a high adsorption capacity, ease of preparation, and the use of low-cost biodegradable domestic waste material makes this material an ideal adsorbent for the removal of total chromium from aqueous solutions. It offers a sustainable and efficient solution for addressing chromium contamination, and its potential as a practical alternative for water treatment is promising.

ACKNOWLEDGMENT

We acknowledge IIMT College of Engineering, Greater Noida, which provided financial support in achieving the various objectives of this research.

REFERENCES

Abdel-Mohsen, A.M., Jancar, J., Kalina, L. and Hassan, A.F. 2020. Comparative study of chitosan and silk fibroin staple microfibers on the removal of chromium (VI): Fabrication, kinetics and thermodynamic studies. Carbohydr. Polym., 234: 115861. https://doi.org/https://doi.org/10.1016/j.carbpol.2020.115861

Adeniyi, A.G., Ighalo, J.O. and Onifade, D.V. 2020. Biochar from the Thermochemical Conversion of Orange Peel and Albedo: Product

Quality and Potential Applications. Chem. Africa, 3: 439-448. https://doi.org/10.1007/s42250-020-00119-6

Ahamad, K.U., Singh, R., Baruah, I. and 2018. Equilibrium and kinetics modeling of fluoride adsorption onto activated alumina, alum, and brick powder. Groundw. Sustain. Dev., 7: 452-458. https://doi.org/https://doi.org/10.1016/j.gsd.2018.06.005

Amin, M. and Chetpattananondh, P. 2019. Biochar from extracted marine Chlorella sp. residue for high-efficiency adsorption with ultrasonication to remove Cr(VI), Zn(II), and Ni(II). Bioresour. Technol., 289: 121578. https://doi.org/https://doi.org/10.1016/j.biortech.2019.121578

Andrade, T.S., Vakros, J., Mantzavinos, D. and Lianos, P. 2020. Biochar obtained by carbonization of spent coffee grounds and its application in the construction of an energy storage device. Chem. Eng. J. Adv., 4: 100061. https://doi.org/https://doi.org/10.1016/j.ceja.2020.100061

Anthony, E.T., Alfred, M.O., Saliu, T.D. and Oladoja, N.A. 2021. One-pot thermal synthesis of Ceria/Montmorillonite composite for the removal of hexavalent chromium from aqueous system. Surf. Interf., 22: 100914. https://doi.org/https://doi.org/10.1016/j.surfin.2020.100914

Bagheri, A., Abu-Danso, E., Iqbal, J. and Bhatnagar, A. 2020. Modified biochar from Moringa seed powder for the removal of diclofenac from aqueous solution. Environ. Sci. Pollut. Res., 27: 7318-7327. https://doi.org/10.1007/s11356-019-06844-x

Bai, C., Wang, L. and Zhu, Z. 2020. Adsorption of Cr(III) and Pb(II) by graphene oxide/alginate hydrogel membrane: Characterization, adsorption kinetics, isotherm and thermodynamics studies. Int. J. Biol. Macromol., 147: 898-910. https://doi.org/https://doi.org/10.1016/j.ijbiomac.2019.09.249

Bedada, D., Angassa, K. and Tiruneh, A. 2020. Chromium removal from tannery wastewater through activated carbon produced from Parthenium hysterophorus weed. Energy, Ecol. Environ., 5: 184-195. https://doi.org/10.1007/s40974-020-00160-8

Benjelloun, M., Miyah, Y. and Akdemir Evrendilek, G. 2021. Recent advances in adsorption kinetic models: Their application to dye types. Arab. J. Chem., 14: 103031. https://doi.org/https://doi.org/10.1016/j.arabjc.2021.103031

Birhanu, Y., Leta, S. and Adam, G. 2020. Removal of chromium from synthetic wastewater by adsorption onto Ethiopian low-cost Odaracha adsorbent. Appl. Water Sci., 10: 227. https://doi.org/10.1007/s13201-020-01310-3

Chakraborty, R., Verma, R. and Asthana, A. 2021. Adsorption of hazardous chromium (VI) ions from aqueous solutions using modified sawdust: kinetics, isotherm and thermodynamic modeling. Int. J. Environ. Anal. Chem., 101: 911-928. https://doi.org/10.1080/03067319.2019.1673743

Chakraborty, V. and Das, P. 2023. Synthesis of nano-silica-coated biochar from thermal conversion of sawdust and its application for Cr removal: kinetic modeling using linear and nonlinear method and modeling using artificial neural network analysis. Biomass Convers. Bioref., 13: 821-831. https://doi.org/10.1007/s13399-020-01024-1

Chen, X., Lam, K.F. and Yeung, K.L. 2011. Selective removal of chromium from different aqueous systems using magnetic MCM-41 nanosorbents. Chem. Eng. J., 172: 728-734. https://doi.org/https://doi.org/10.1016/j.cej.2011.06.042

Dan, S. and Chattree, A. 2018. Sorption of fluoride using chemically modified *Moringa oleifera* leaves. Appl. Water Sci., 8: 76. https://doi.org/10.1007/s13201-018-0718-6

Dim, P.E., Mustapha, L.S., Termtanun, M. and Okafor, J.O. 2021. Adsorption of chromium (VI) and iron (III) ions onto acid-modified kaolinite: Isotherm, kinetics and thermodynamics studies. Arab. J. Chem., 14: 103064. https://doi.org/https://doi.org/10.1016/j.arabjc.2021.103064

Dong, H., Liang, H. and Yang, L. 2023. Porous biochar derived from waste distiller's grains for hexavalent chromium removal: Adsorption performance and mechanism. J. Environ. Chem. Eng., 11: 110137. https://doi.org/https://doi.org/10.1016/j.jece.2023.110137

GracePavithra, K., Jaikumar, V., Kumar, P.S. and SundarRajan, P. 2019. A review on cleaner strategies for chromium industrial wastewater: Present research and future perspective. J. Clean Prod., 228: 580-593. https://doi.org/https://doi.org/10.1016/j.jclepro.2019.04.117

Gupta, G.K., Ram, M. and Bala, R. 2018. Pyrolysis of chemically treated corncob for biochar production and its application in Cr(VI) removal. Environ. Prog. Sustain. Energy, 37: 1606-1617. https://doi.org/https://doi.org/10.1002/ep.12838

Hackbarth, F.V., Maass, D. and de Souza, A.A.U. 2016. Removal of hexavalent chromium from electroplating wastewaters using marine macroalga *Pelvetia canaliculata* as a natural electron donor. Chem. Eng. J., 290: 477-489. https://doi.org/https://doi.org/10.1016/j.cej.2016.01.070

Hu, H., Zhang, J., Wang, T. and Wang, P. 2022. Adsorption of toxic metal ion in agricultural wastewater by torrefaction biochar from bamboo shoot shell. J. Clean. Prod., 338: 130558. https://doi.org/https://doi.org/10.1016/j.jclepro.2022.130558

Islam, M.A., Angove, M.J. and Morton, D.W. 2019. Recent innovative research on chromium (VI) adsorption mechanism. Environ. Nanotechnol. Monit. Manag., 12: 100267. https://doi.org/https://doi.org/10.1016/j.enmm.2019.100267

Jahangiri, K., Yousefi, N. and Ghadiri, S.K. 2019. Enhancement adsorption of hexavalent chromium onto modified fly ash from aqueous solution; optimization; isotherm, kinetic and thermodynamic study. J. Dispers. Sci. Technol., 40: 1147-1158. https://doi.org/10.1080/01932691.2018.1496841

Jamaluddin, N.S., Alias, N.H. and Samitsu, S. 2022. Efficient chromium (VI) removal from wastewater by adsorption-assisted photocatalysis using MXene. J. Environ. Chem. Eng., 10: 108665. https://doi.org/https://doi.org/10.1016/j.jece.2022.108665

Jeyaseelan, A., Katubi, K.M.M. and Alsaiari, N.S. 2021. Design and fabrication of sulfonic acid functionalized graphene oxide for enriched fluoride adsorption. Diam. Relat. Mater., 117: 108446. https://doi.org/https://doi.org/10.1016/j.diamond.2021.108446

Karimi-Maleh, H., Ayati, A. and Ghanbari, S. 2021. Recent advances in removal techniques of Cr(VI) toxic ion from aqueous solution: A comprehensive review. J. Mol. Liq., 329: 115062. https://doi.org/https://doi.org/10.1016/j.molliq.2020.115062

Kassimu, H., Sallau, A.B. and Nzelibe, H.C. 2022. Hexavalent chromium (Cr VI) bioreduction potential of anthocyanins rich extract of watermelon (*Citrullus lanatus*) rind. Chem. Africa, 5: 1837-1844. https://doi.org/10.1007/s42250-022-00504-3

Khalifa, E.B., Azaiez, S. and Magnacca, G. 2023. Synthesis and characterization of promising biochars for hexavalent chromium removal: application of response surface methodology approach. Int. J. Environ. Sci. Technol., 20: 4111-4126. https://doi.org/10.1007/s13762-022-04270-0

Liu, N., Zhang, Y. and Xu, C. 2020. Removal mechanisms of aqueous Cr(VI) using apple wood biochar: a spectroscopic study. J. Hazard. Mater., 384: 121371. https://doi.org/https://doi.org/10.1016/j.jhazmat.2019.121371

Mallik, A.K., Moktadir, M.A. and Rahman, M.A. 2022. Progress in surface-modified silicas for Cr(VI) adsorption: A review. J. Hazard. Mater., 423: 127041. https://doi.org/https://doi.org/10.1016/j.jhazmat.2021.127041

Mohanty, S., Benya, A. and Hota, S. 2023. Eco-toxicity of hexavalent chromium and its adverse impact on the environment and human health in Sukinda Valley of India: A review on pollution and prevention strategies. Environ. Chem. Ecotoxicol., 5: 46-54. https://doi.org/https://doi.org/10.1016/j.enceco.2023.01.002

Mpelane, S., Mketo, N., Bingwa, N. and Nomngongo, P.N. 2022. Synthesis of mesoporous iron oxide nanoparticles for adsorptive removal of levofloxacin from aqueous solutions: Kinetics, isotherms, thermodynamics, and mechanism. Alexandria Eng. J., 61: 8457-8468. https://doi.org/https://doi.org/10.1016/j.aej.2022.02.014

Nur-E-Alam, M., Mia, M.A.S., Ahmad, F. and Rahman, M.M. 2020. An overview of chromium removal techniques from tannery effluent. Appl. Water Sci., 10: 205. https://doi.org/10.1007/s13201-020-01286-0

Pap, S., Bezanovic, V. and Radonic, J. 2018. Synthesis of highly efficient functionalized biochars from fruit industry waste biomass for the removal of chromium and lead. J. Mol. Liq., 268: 315-325. https://doi.org/https://doi.org/10.1016/j.molliq.2018.07.072

Perraki, M., Vasileiou, E. and Bartzas, G. 2021. Tracing the origin of chromium in groundwater: Current and new perspectives. Curr. Opin. Environ. Sci., *22*: 100267

Qiu, Y., Zhang, Q. and Gao, B. 2020. Removal mechanisms of Cr(VI) and Cr(III) by biochar supported nanosized zero-valent iron: Synergy of adsorption, reduction and transformation. Environ. Pollut., 265: 115018. https://doi.org/https://doi.org/10.1016/j.envpol.2020.115018

Rajapaksha, A.U., Alam, M.S. and Chen, N. 2018. Removal of hexavalent chromium in aqueous solutions using biochar: Chemical and spectroscopic investigations. Sci. Total Environ., 625: 1567-1573. https://doi.org/https://doi.org/10.1016/j.scitotenv.2017.12.195

Revellame, E.D., Fortela, D.L. and Sharp, W. 2020. Adsorption kinetic modeling using pseudo-first order and pseudo-second order rate laws: A review. Clean Eng. Technol., 1: 100032. https://doi.org/https://doi.org/10.1016/j.clet.2020.100032

Sarkar, A., Ranjan, A. and Paul, B. 2019. Synthesis, characterization, and application of surface-modified biochar synthesized from rice husk, an agro-industrial waste, for the removal of hexavalent chromium from drinking water at near-neutral pH. Clean Technol. Environ. Policy, 21: 447-462. https://doi.org/10.1007/s10098-018-1649-5

Shakya, A., Núñez-Delgado, A. and Agarwal, T. 2019. Biochar synthesis from sweet lime peel for hexavalent chromium remediation from aqueous solution. J. Environ. Manage., 251: 109570. https://doi.org/https://doi.org/10.1016/j.jenvman.2019.109570

Srivastava, A., Dave, H. and Azad, S.K. 2021a. Iron Modification of Biochar Developed from Tectona grandis Linn. F. for Adsorptive Removal of Tetracycline from Aqueous Solution. Anal. Chem. Lett., 11: 360-375. https://doi.org/10.1080/22297928.2021.1934113

Srivastava, A., Dave, H. and Prasad, B. 2022a. Adsorptive behavior of L-Arginine-silica micro-particles against arsenic and fluoride in aqueous solution. Environ Nanotechnology, Monit Manag., 17: 100636. https://doi.org/https://doi.org/10.1016/j.enmm.2021.100636

Srivastava, A., Dave, H. and Prasad, B. 2022b. Low-cost iron-modified Syzygium cumini l. Wood biochar for adsorptive removal of ciprofloxacin and doxycycline antibiotics from aqueous solution. Inorg Chem Commun., 144: 109895. https://doi.org/https://doi.org/10.1016/j.inoche.2022.109895

Srivastava, A., Kumar, S. and Kavita, A. 2022c. Arsenite and arsenate ions adsorption onto a biogenic nano-iron entrapped dual network Fe @ alginate - □ - carrageenan hydrogel beads. Nanotechnol Environ Eng. https://doi.org/10.1007/s41204-022-00280-y

Srivastava, A., Kumari, M. and Prasad, K.S. 2021b. Hydrogel beads containing ginger extract mediated nano-zirconium as an adsorbent for fluoride removal from aqueous solution. Int. J. Environ. Anal. Chem., 1-15. https://doi.org/10.1080/03067319.2021.1877282

Srivastava, A., Kumari, M. and Ramanathan, A. 2020. Removal of fluoride from aqueous solution by mesoporous silica nanoparticles functionalized with chitosan derived from mushroom. J. Macromol. Sci. Part A, 57: 619-627. https://doi.org/10.1080/10601325.2020.1738896

Srivastava, A., Selvaraj, K. and Prasad, K.S. 2019. Nanoparticles Based Adsorbent for Removal of Arsenic from Aqueous Solution. Asian J. Water, Environ. Pollut., 16: 87-93. https://doi.org/10.3233/AJW-190046

Staszak, K., Kruszelnicka, I. and Ginter-Kramarczyk, D. 2023. Advances in the Removal of Cr(III) from Spent Industrial Effluents-A Review. Materials (Basel), 16.

Tangestani, M., Naeimi, B. and Dobaradaran, S. 2022. Biosorption of fluoride from aqueous solutions by Rhizopus oryzae: Isotherm and kinetic evaluation. Environ. Prog. Sustain. Energy, 41: e13725. https://doi.org/10.1002/ep.13725.

Ugwu, E.I. and Agunwamba, J.C. 2020. A review of the applicability of activated carbon derived from plant biomass in the adsorption of chromium, copper, and zinc from industrial wastewater. Environ. Monit. Assess., 192: 240. https://doi.org/10.1007/s10661-020-8162-0.

Vaiopoulou, E. and Gikas, P. 2020. Regulations for chromium emissions to the aquatic environment in Europe and elsewhere. Chemosphere, 254: 126876. https://doi.org/10.1016/j.chemosphere.2020.126876.

Vasileiou, E., Papazotos, P. and Dimitrakopoulos, D., Perraki, M. 2019. Expounding the origin of chromium in groundwater of the Sarigkiol basin, Western Macedonia, Greece: a cohesive statistical approach and hydrochemical study. Environ. Monit. Assess., 191: 509. https://doi.org/10.1007/s10661-019-7655-1.

Wan, Y., Luo, H. and Cai, Y. 2023. Selective removal of total Cr from a complex water matrix by chitosan and biochar modified-FeS: Kinetics and underlying mechanisms. J. Hazard. Mater., 454: 131475. https://doi.org/10.1016/j.jhazmat.2023.131475.

Yadav, K., Latelwar, S.R., Datta, D. and Jana, B. 2023. Efficient removal of MB dye using litchi leaves powder adsorbent: Isotherm and kinetic studies. J. Indian Chem. Soc., 100: 100974. https://doi.org/10.1016/j.jics.2023.100974.

Yahya, M.D., Obayomi, K.S. and Abdulkadir, M.B. 2020. Characterization of cobalt ferrite-supported activated carbon for removal of chromium and lead ions from tannery wastewater via adsorption equilibrium. Water Sci. Eng., 13: 202-213. https://doi.org/10.1016/j.wse.2020.09.007.

Yusuff, A.S. 2019. Adsorption of hexavalent chromium from aqueous solution by Leucaena leucocephala seed pod activated carbon: equilibrium, kinetic and thermodynamic studies. Arab J. Basic Appl. Sci., 26: 89-102. https://doi.org/10.1080/25765299.2019.1567656.

Zhao, J., Yu, L. and Ma, H. 2020. Corn stalk-based activated carbon synthesized by a novel activation method for high-performance adsorption of hexavalent chromium in aqueous solutions. J. Colloid Interf. Sci., 578: 650-659. https://doi.org/10.1016/j.jcis.2020.06.031.

Zhao, N., Yin, Z. and Liu, F. 2018. Environmentally persistent free radicals mediated removal of Cr(VI) from highly saline water by corn straw biochars. Bioresour. Technol., 260: 294-301. https://doi.org/10.1016/j.biortech.2018.03.116.

Zolfi Bavariani, M., Ronaghi, A. and Ghasemi, R., 2019. Influence of pyrolysis temperatures on FTIR analysis, nutrient bioavailability, and agricultural use of poultry manure biochars. Commun. Soil Sci. Plant Anal., 50: 402-411. https://doi.org/10.1080/00103624.2018.1563101.

ORCID DETAILS OF THE AUTHORS

Anushree Srivastava: https://orcid.org/0000-0003-0056-4511